

PAPER

# The effect of load and addition of MWCNTs on silicone based TIMs on thermal contact heat transfer across Cu/Cu interface

To cite this article: Ramakrishna Devananda P and K NarayanPrabhu 2019 *Mater. Res. Express* **6** 1165h9

View the [article online](#) for updates and enhancements.

## Recent citations

- [Influence of thermal contact resistance of cementing interface on radial heat transfer in wellbore](#)  
Yunxing Duan and Hao Yang



The banner features a dark blue background with a satellite view of Earth. On the left, there are three circular logos: the top one is 'ECS' (Electrochemical Society), the middle one is 'The Electrochemical Society' with a stylized 'ECS' logo, and the bottom one is 'THE KOREAN ELECTROCHEMICAL SOCIETY'. The central text reads 'Joint International Meeting PRiME 2020 October 4-9, 2020' in white and blue. Below this, a blue bar contains the text 'Attendees register at NO COST!' in white. On the right side, there is a large white 'PRIME' logo with 'TM' and 'PACIFIC RIM MEETING ON ELECTROCHEMICAL AND SOLID STATE SCIENCE' underneath, followed by '2020' in large white numbers. At the bottom right, a blue bar contains the text 'REGISTER NOW' in white with a right-pointing arrow.



## PAPER

## The effect of load and addition of MWCNTs on silicone based TIMs on thermal contact heat transfer across Cu/Cu interface

RECEIVED  
17 July 2019REVISED  
6 October 2019ACCEPTED FOR PUBLICATION  
29 October 2019PUBLISHED  
8 November 2019Ramakrishna Devananda P<sup>1,2,4</sup> and K NarayanPrabhu<sup>3</sup> <sup>1</sup> Asst Professor, Department of Mechanical Engineering, Sahyadri College of Engineering and Management, Mangaluru 575009, India<sup>2</sup> Research Scholar, Department of Metallurgical and Materials Engineering, National Institute of Technology Karnataka, Surathkal, Mangaluru 575025, India<sup>3</sup> Professor, Department of Metallurgical and Materials Engineering, National Institute of Technology Karnataka, Surathkal, Mangaluru 575025, India<sup>4</sup> Visvesvaraya Technological University Belagavi, Karnataka, IndiaE-mail: [knprabhu.nitk@gmail.com](mailto:knprabhu.nitk@gmail.com)**Keywords:** thermal contact resistance, heat transfer, thermal interface material, MWCNT, silicone grease, thermal interface**Abstract**

In the present work, the effect of thermal interface material (TIM) and load on contact heat transfer between hot and cold cylindrical copper specimens was assessed. Pristine silicone grease and multi walled carbon nanotubes (MWCNT) impregnated silicone grease was used as TIM. Copper specimens with L/D ratios of 1 and 5 were used. For copper specimens with L/D ratio of 1, the interfacial heat transfer was quantified by estimating the peak heat flux and integral heat flow using a lumped heat capacitance approach. An inverse solution to heat conduction equation was adopted for estimating heat flux transients for copper specimens with L/D ratio of 5. As the applied load increased from a no load condition to 5 kg, the peak heat flux and the corresponding integral flow increased significantly. Increasing the load above 5 kg did not result in any significant changes in the peak heat flux and integral heat flow for both sets of specimens. The effect of load on the contact heat transfer was significant in the absence of TIM. The use of 0.1 wt% MWCNT- silicone grease as TIM significantly increased the heat flow for no load condition. At higher loads, the effect of MWCNT was insignificant and caused deterioration in the heat flow parameters. Further, increasing the MWCNT content to 1 wt% in silicone grease decreased the heat flux transients at all loading conditions. The thermal contact resistance ( $R_T$ ) was calculated and it increased exponentially with the peak temperature difference ( $\Delta T_{\max}$ ) between hot and cold specimens irrespective of the L/D ratio.

**Nomenclature**

TIM	Thermal interface material
SG	Silicone Grease
CNT	Carbon nanotube
MWCNT	Multi walled carbon nanotube
$R_T$	Thermal contact resistance ( $\text{cm}^2\text{C W}^{-1}$ )
PTFE	Polytetrafluoroethylene
$\Delta T_{\max}$	Peak temperature difference ( $^{\circ}\text{C}$ )
$k$	Thermal conductivity ( $\text{W m}^{-1}\text{K}^{-1}$ )
RT	Room temperature ( $^{\circ}\text{C}$ )
BLT	Bond line Thickness
$q$	heat flux ( $\text{W m}^{-2}$ )

$C_p$	specific heat ( $\text{J kg}^{-1}\text{K}^{-1}$ )
$V$	volume of the specimen ( $\text{m}^3$ )
$A$	cross sectional area of the specimen ( $\text{m}^2$ )
$\frac{dT}{dt}$	Cooling rate ( $^{\circ}\text{C s}^{-1}$ )
$\Theta$	Dimensionless temperature
$L$	Length of the specimen (mm)
$D$	Diameter of the specimen (mm)
NL	No load

## Introduction

Thermal management has become an important aspect in areas where efficient removal of heat is necessary for enhanced performance and improved reliability [1]. The advent of miniaturised products especially in the field of electronics has made thermal management even more challenging as miniaturization leads to the generation of enormous amounts of heat [2, 3]. The heat generated needs to be efficiently removed in order to keep the operating temperatures well within the safe limits [4]. Studies have shown that achieving lower operating temperatures by efficient transfer of heat results in positive impact on the device life and further leads to reduced power dissipation and higher processing speeds [5]. One of the impediments to the efficient transfer of heat is the existence of interface between the heat generating package (heat source) and the heat sink. The interface between the heat source and the heat sink gives rise to thermal contact resistance owing to surface roughness and non flatness, resulting in limited contact between them at discrete points [6]. Thus, apart from the discrete points where there is an actual contact, interfaces are characterised by significant presence of voids filled with poor thermally conductivity air ( $k = 0.026 \text{ W m}^{-1} \text{ K}^{-1}$  at RT) [6, 7]. The presence of air increases the thermal contact resistance and hence the heat transfer across the interface decreases.

Abdullah *et al* [8] conducted experimental studies on the effect of pressure on thermal contact resistance. It was found that, when the specimens were subjected to increasing pressure, the contact resistance reduced significantly. Hence, one of the methods to enhance the heat transfer across the interface could be by increasing the pressure. The application of pressure results in crushing of peaks resulting in enhanced heat transfer owing to the increased contact area [9]. However, load constraints curtail employing higher pressures in many practical applications [6, 9]. Studies have also shown that the effect of pressure depends on the material of the test surfaces used. Tariq *et al* [10] studied the thermal contact heat transfer across interfaces. In their study, they used copper, stainless steel and brass specimens. It was found that the thermal contact conductance increased with increasing pressure. The study also reported that with copper the degree of improvement in thermal contact conductance was maximum and the improvement was the lowest with stainless steel. This was due to the fact that the yield strength of stainless is highest which resulted in lower degree of deformation. Higher degree of deformation would result in enhanced contact area and thereby enhancing the thermal contact conductance. The second method by which thermal contact resistance could be reduced is by employing highly polished interfacial surfaces. However, this method of employing polished surfaces has limited practical feasibility owing to the increased cost [6, 9]. The effective way of improving heat transfer across the interface would be by introducing a thermal conductive TIM between the heat source and the heat sink. The application of TIMs results in enhanced heat transfer, as air gets replaced with the TIMs at the interface [11]. Yovanovich *et al* [12] found that for bare interfaces the joint resistance at a pressure range of 0.007 to 0.35 MPa was in the range of 2.665 to  $1.903 \text{ cm}^2\text{C/W}$ . However, with the introduction of silicone grease, the joint resistance reduced to a range of 0.335 to  $0.213 \text{ cm}^2\text{C/W}$ . Thus, the introduction of silicone grease reduced thermal resistance significantly as the interstitial air which is a poor conductor of heat was replaced by silicone grease at the interface resulting. The replacement of air and subsequent filling of grease leads to effective thermal paths [13]. Apart from possessing high thermal conductivity ( $k$ ), an ideal TIM should possess characteristics such as easy deformability, minimal thickness, excellent wetting, non toxicity, non corrosive, long term stability, easy to apply, economical and should be able to withstand mechanical stress [6, 9, 14, 15].

The introduction of TIMs at the interface would result in thermal resistance across the interface and is computed as follows [16]

$$\text{Thermal resistance} = (BLT/k_{\text{TIM}}A) + R_{c1} + R_{c2} \quad (1)$$

Equation (1) shows that the thermal contact resistance depends on the parameters and properties that include, thermal conductivity ( $k$ ) of the interface material, bondline thickness (BLT), area of contact, contact resistance

( $R_{c1} + R_{c2}$ ) that exists between interface material and two contacting surfaces. Further, the pressure, surface roughness, compressive modulus and surface flatness [14] also influence the contact resistance.

Several types of TIMs are used in practical applications. These include thermal grease, PCMs, pads, solders and thermal adhesives [7, 17]. Thermal greases owing to some of their inherent advantages like ability to reach thin BLT with minimum application of pressure and lower viscosity values [18] are commonly used as TIMs. Thermal grease is a kind of thixotropic paste having higher conductivity fillers dispersed in a medium of silicone or hydrocarbon oil [19, 20]. The addition of fillers increases thermal conductivities of TIMs, thus making them more efficient in meeting the requirements of advanced thermal applications [21]. Metal, ceramic or carbon based additives are commonly used as fillers [7]. Metal based thermal grease/paste use metals like Cu, Al, Ag as fillers, whereas ceramic based thermal grease employ ceramic fillers such as beryllium oxide, zinc oxide, aluminium nitride etc. Further, thermal grease based on carbon employ CNTs and carbon nanofibres as fillers [19]. Some of the disadvantages include contamination caused owing to flow out of the grease from the interface area and difficulty in controlling the thickness. Further, thermal grease dry out with time resulting in loss of thermal path [14, 18].

Sartre *et al* [3] conducted investigations on thermal contact resistance between copper specimens and aluminium plate. The suitability of various interstitial materials including grease, PCM coated foils, metallic foils and silicone foils were studied. It was reported that, on application of G641 grease (silicone grease) the thermal contact resistance was  $1.47 \times 10^{-4} \text{ m}^2 \text{ kW}^{-1}$ , whereas, for bare junction the thermal contact resistance was reported to be  $6.67 \times 10^{-4} \text{ m}^2 \text{ kW}^{-1}$ . The study used enhancement factor (E), a dimensionless parameter, to evaluate interstitial materials, with higher E values indicating better performing materials. Among various interstitial tested, greases exhibited highest enhancement factor. Gowda *et al* [22] conducted silicone grease reliability testing. In their study, five different combinations of silicone based greases with two different filler systems were used. The experiments were conducted for three pressure conditions viz. 15 psi, 30 psi and 45 psi. It was found that, as filler loading increases, the thermal conductivity also increased. It was reported that the viscosity increased with increasing the filler loading which in turn caused the BLT to increase. The study also revealed that, at a low pressure of 15 psi, greases with higher filler contents underperformed when compared to grease with lower filler loading despite the thermal conductivity of the former being higher. This was attributed to the fact that, the BLT of greases with higher content was higher at low pressure values. However, increasing the pressure to higher values resulted in reduction of thermal resistance of silicone greases with higher filler when compared to silicone grease with lower filler content.

Several researchers [15, 23, 24] reported the effect of addition of CNTs on silicone grease TIM. The advantages of CNTs include higher thermal conductivity ( $>3000 \text{ W mK}^{-1}$ ) and larger aspect ratio that enables percolation network at low fractions [7]. Yujun *et al* [15] studied the effect of addition of MWCNTs on thermal grease. The study found that short MWCNTs results in increased thermal performance. It was also reported that the surface modification of MWCNTs caused reduced entanglement of MWCNTs resulting in enhanced performance. Further, the study revealed that, as the contact pressure was increased, the thermal resistance decreased with short and surface modified MWCNTs as they are less sensitive to the contact pressure. Chen *et al* [23] reported that the application carboxylated CNTs to silicone grease resulted in 35% reduction in thermal resistance value when compared to pristine silicone. The study reported thermal resistance as low as  $0.18 \times 10^{-4} \text{ m}^2 \text{ kW}^{-1}$  when 2 wt% CNT-COOH was applied at the interface. Fabris *et al* [24] studied the effect of addition of CNTs on commercial TIM (ArticSilver<sup>®</sup> 5-AS) and silicone oil under steady state conditions. The study reported that the addition of CNTs in commercial TIM results in enhanced thermal resistance resulting in reduced performance. The study also found that increased CNT concentration resulted in higher thermal resistance value owing to thickening of interface material causing difficulty in spreading. However, the addition of CNTs in silicone oil at higher pressure resulted in improved performance.

Majority of the work, in the field of TIMs are carried out under steady state conditions. The suitability of TIMs under transient conditions is seldom studied. The tests that employ transient approach are expensive and are difficult to conduct but offer advantages that include shorter test duration and estimation of heat flux transients and other heat flow parameters [10, 25]. Further, in most of the applications, the characteristics of heat flow at the onset of process determine the effectiveness of heat transfer [25]. Hence it is of foremost importance to understand the process of heat transfer under transient conditions. In the present work, an apparatus has been designed and fabricated with an objective of estimating thermal performance parameters under transient conditions. The study deals with the evaluation of the performance of silicone based grease as TIMs under various loading conditions for Cu-Cu interface. The effect of addition of pristine CNTs to silicon grease on contact heat transfer was also investigated. The heat flux transients were estimated by adopting lumped heat capacitance approach and inverse method for specimens with L/D ratio of 1 and 5 respectively.

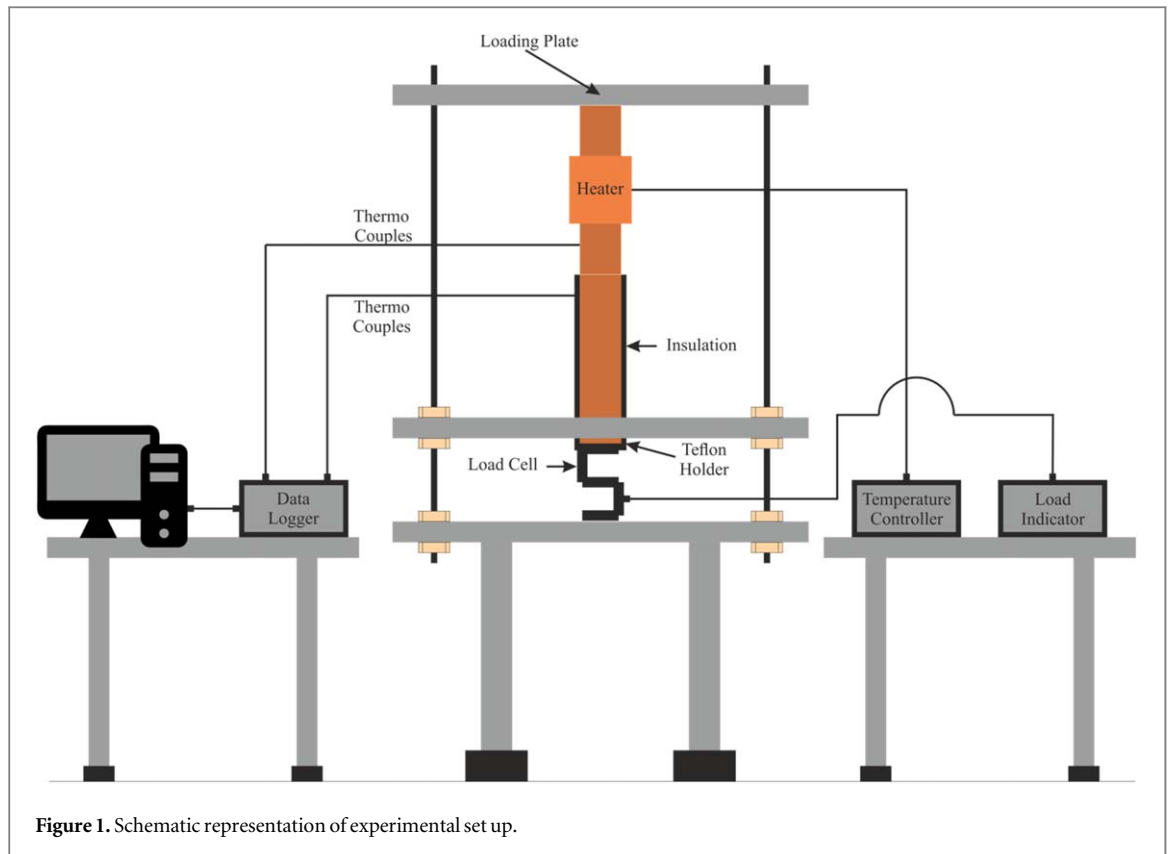


Figure 1. Schematic representation of experimental set up.

## Methodology

The experiments were conducted by placing the TIM at the interface between two cylindrical specimens. Figure 1 shows the schematic sketch of the experimental set-up for estimating heat flux transients. The specimens were placed on a PTFE holder which in turn was placed over a load cell (Epoch Instruments and controls Pvt. Ltd, Model No: LZYB, Capacity: 0–200 kg). The load cell was used to measure the load that was applied on to the specimens. The load cell is mounted on a flat plate and is connected to a microcontroller based digital indicator (Epoch Instruments and controls Pvt. Ltd, Model No: SM-12, Excitation voltage 5 VDC ( $\pm 1\%$ )). The accuracy of the load indicator was  $\pm 0.01\%$  of the full scale with the minimum bridge resistance of  $85\Omega$ . The load was applied by placing plates of known weights on the top of the upper specimen. The set up consist of four pillars that facilitate the placement of plates over specimens at appropriate alignment. The experiments were conducted for two sets of cylindrical specimens of copper. In each of the sets, the upper specimen with the heater acted as the heat source and the lower specimen was the heat sink. The heating was done by a mica strip heater (150 kW, 250 V) which was attached to the upper specimen. The mica strip heater was connected to a temperature regulator which allowed the user to regulate or set the temperatures to a preset value. The source and sink were instrumented with a mineral insulated sheathed K-type thermocouple of 1 mm diameter. The thermocouples were instrumented by drilling holes in to the specimens at the appropriate locations through EDM technique. The dimensions of the first set with L/D ratio of 1 was  $\phi 25 \times 25$  mm and the dimensions of the second set with L/D ratio of 5 was  $\phi 25 \times 125$  mm. The schematic diagrams of the first and second sets of specimens are shown in figures 2 and 3 respectively. In both cases, the source was heated to a temperature of  $75 \pm 2^\circ\text{C}$  and the corresponding changes in temperature in the lower specimen were recorded. To maximize heat transfer in the axial direction, the lower specimens were insulated with PTFE tape and cerawool material. The acquisition of the variation of temperature with time was accomplished by using a data logger (NI 9213) which was connected to thermocouples using compensating cables. The data logger was in turn interfaced to a computer.

For specimens with L/D ratio of 1, the source was instrumented with the thermocouples at 3 mm and 6 mm, whereas the sink was instrumented with thermocouples at 3 mm and 15 mm. The temperature data was acquired at every 0.1 s using data logger. The heat flux was calculated by employing lumped capacitance approach since there was no temperature gradient within the sink. Lumped heat capacitance method assumes negligible temperature gradients and the temperature is considered to be uniform within the specimen material [26].

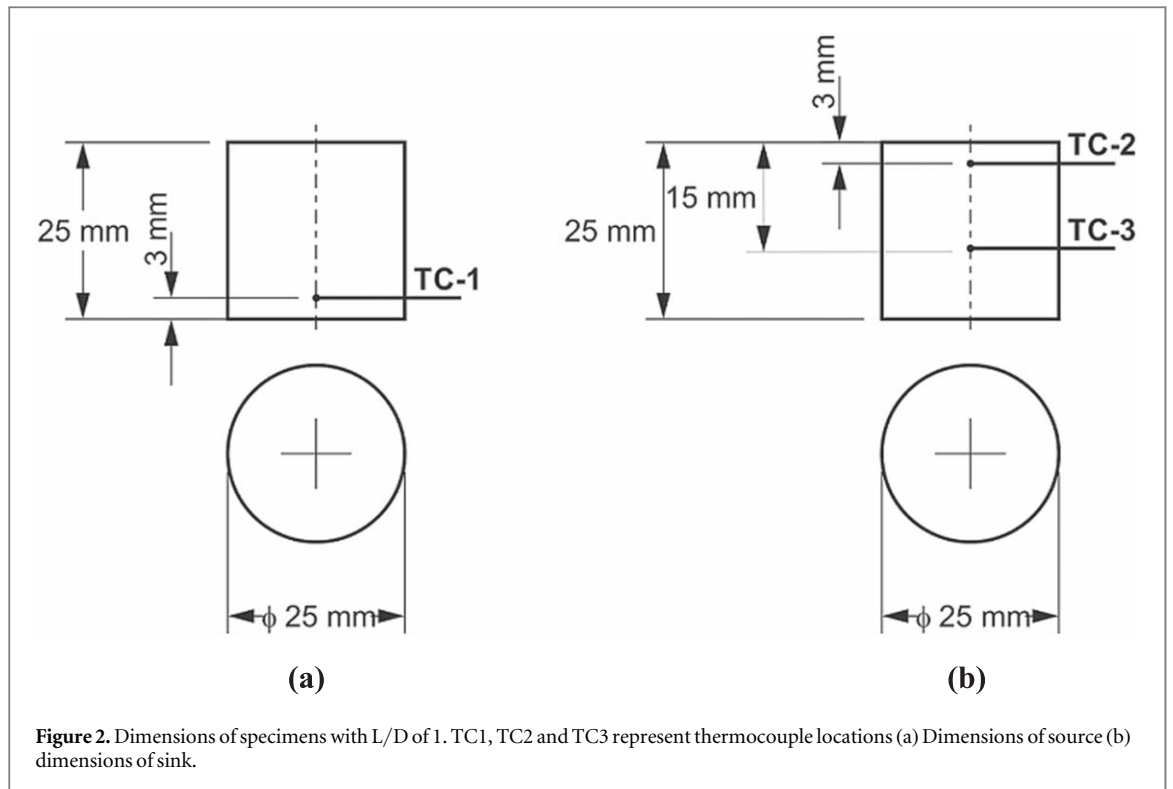


Figure 2. Dimensions of specimens with L/D of 1. TC1, TC2 and TC3 represent thermocouple locations (a) Dimensions of source (b) dimensions of sink.

Thus,

$$q = \rho C_p (V/A) \frac{dT}{dt} \tag{2}$$

where

q is the heat flux

$C_p$  is the specific heat

V is the specimen volume

A is the area normal to the heat flow direction

$\frac{dT}{dt}$  is the cooling rate.

For specimens with length to diameter ratio of 5 ( $\phi 25 \times 125$  mm), the source was instrumented with thermocouples at 2 mm and 50 mm from the interface whereas the sink was instrumented with thermocouples at 2 mm, 14 mm and 111 mm from the interface. The temperature data was acquired at every 1 s and the peak heat flux was estimated through inverse heat conduction approach as there was significant temperature gradient. Inverse heat conduction approach utilizes the knowledge of interior temperature history to determine the unknown boundary conditions like heat flux, surface temperature and other interfacial heat parameters [10, 26, 27].

The heat flux transients in the case of specimens with length to diameter ratio of 5 were estimated. Since, the heat transfer along the radial direction was negligible, one dimensional inverse heat conduction problem was solved using Beck's non linear estimation technique [28]. The one dimensional heat conduction ,

$$\frac{\partial}{\partial x} \left( k \frac{\partial T}{\partial x} \right) = \rho C_p \left( \frac{\partial T}{\partial t} \right) \tag{3}$$

was solved by considering following boundary conditions

$$k \frac{\partial T}{\partial x} \Big|_{X=0} = q \text{ (where X is the distance from the interface)}$$

$$k \frac{\partial T}{\partial x} \Big|_{X=L} = 0$$

$$T(X, 0) = 25 \text{ }^\circ\text{C (Initial condition)}$$

The inverse model used the temperature measured by thermocouples at locations TC-2, TC-3 and TC-4 positioned at 2 mm, 14 mm and 111 mm (from the interface) of the cold body (lower specimen) respectively. Inverse algorithm requires minimization of objective function  $f(q)$ .

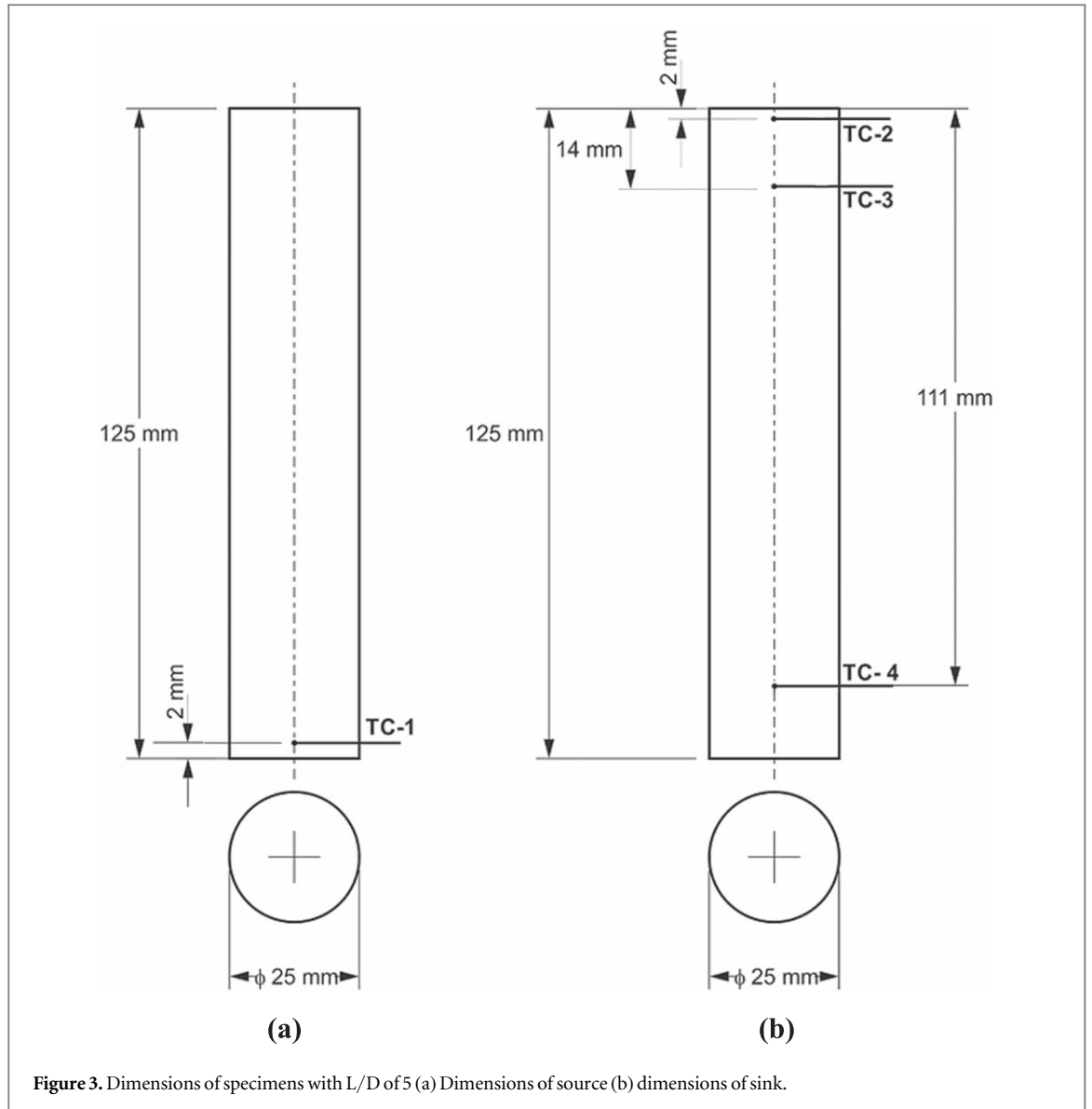


Figure 3. Dimensions of specimens with L/D of 5 (a) Dimensions of source (b) dimensions of sink.

$$f(q) = \sum_{i=1}^n \sum_{j=1}^{m+1} (T(L_i, t + (j - 1)\Delta t) - Y_i)^2 \tag{4}$$

The objective function  $f(q)$  is defined as the summation of square of difference between measured and calculated temperatures. Thus, the heat flux ( $q$ ) at the unknown boundary ( $X = 0$ ) was estimated by minimizing equation (4)

where,  $n$  is the number of positions where thermocouples are located ( $n = 3$ )

$m$  is the total number of future time steps ( $m = 4$ )

Similarly,  $Y_i$  represents the measured temperature at the  $i^{\text{th}}$  location,

$T$  represents the calculated temperature,

$L_i$  is the thermocouple location,

$t$  is the time

$\Delta t$  is the time step increment ( $\Delta t = 1$  s).

The temperature increment at  $i^{\text{th}}$  thermocouple location and  $j-1^{\text{th}}$  future time step was calculated for an increment of 1% of  $q^{l-1}(t)$ . Further, the heat flux increment  $\Delta q^l(t)$  for minimizing objective function was calculated as shown in equation (5).

$$\Delta q^l(t) = \frac{\sum_{i=1}^n \sum_{j=1}^{m+1} (T^{l-1}(L_i, t + (j - 1)\Delta t) - Y_i) \varphi_{i,j}^{l-1}}{\sum_{i=1}^n \sum_{j=1}^{m+1} (\varphi_{i,j}^{l-1})^2} \tag{5}$$

In the above equation  $\varphi_{i,j}$  is sensitivity coefficient. The sensitivity coefficient signifies the effect on estimated temperature resulting due to small changes in the heat flux ( $q$ ). The above equation (5) is obtained by equating the first derivative of equation (4) to zero and subsequently combining the Taylor's series of expansion of

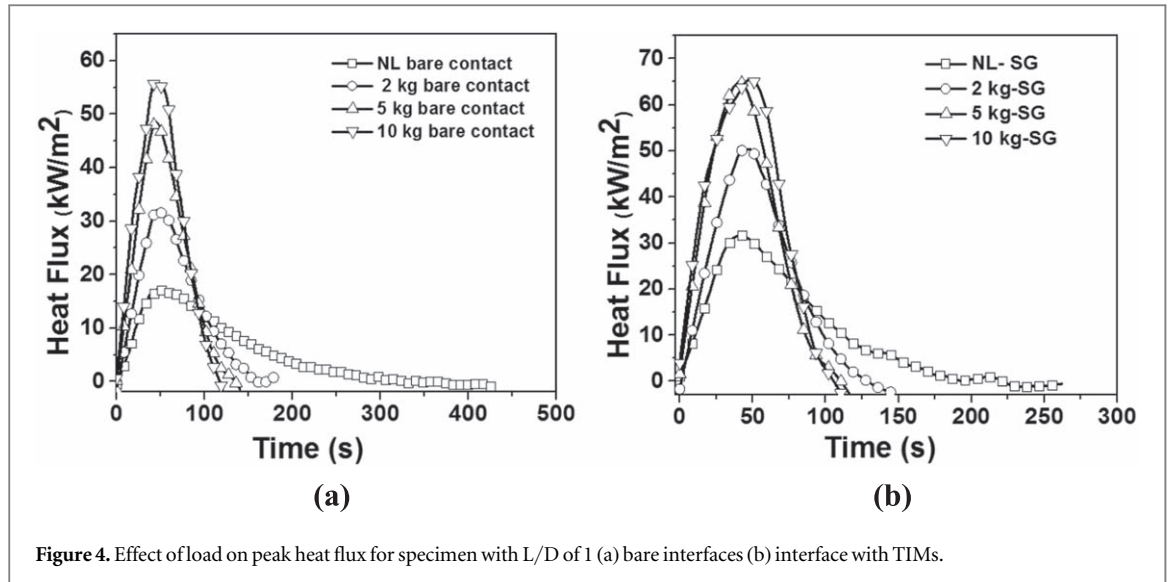


Figure 4. Effect of load on peak heat flux for specimen with L/D of 1 (a) bare interfaces (b) interface with TIMs.

temperature dependent heat flux. The heat flux  $q$  is calculated as,

$$q^l(t) = q^{l-1}(t) + \Delta q^l(t) \quad (6)$$

The objective function is optimized at each time step by iteratively calculating heat flux using equations (5)–(6). The convergence limit for terminating the iterative algorithm was obtained when

$$[(\Delta q^l(t)/q^l(t))] < 10^{-6} \quad (7)$$

A detailed methodology of the solution of inverse heat conduction problems is given in ref. [26, 28].

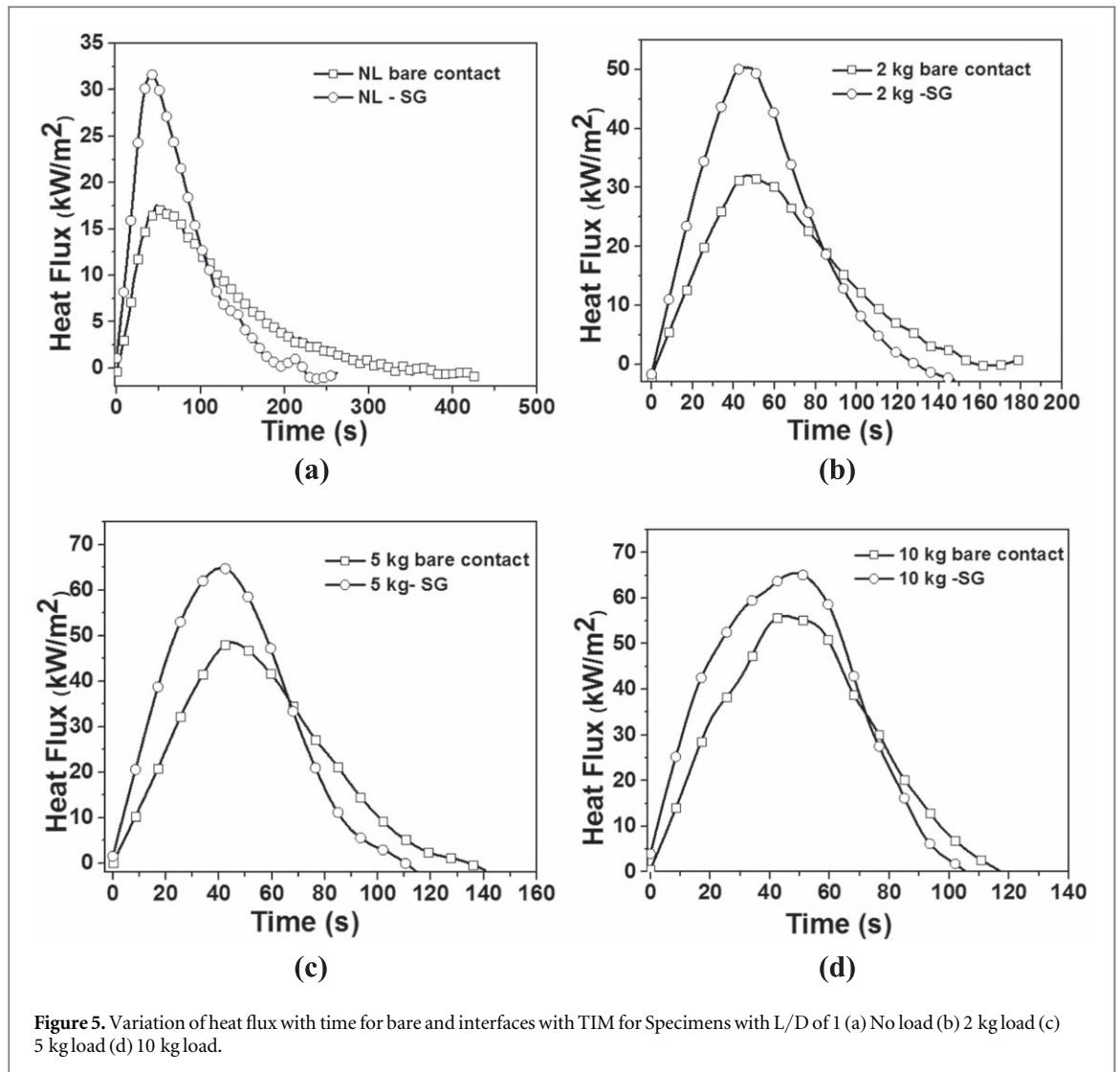
Commercially available silicone grease (Metroarc 211 compound from Wacker Metroark Chemicals Pvt. Ltd Kolkata) was used as TIM. The effect of MWCNT addition on thermal interface material was studied by adding MWCNT to silicone grease. The as-received MWCNT (diameter 10 nm–25 nm, Length 300–500 nm, Chengdu Organic Chemical Co Ltd, Chinese Academy of Science, China) was dispersed in silicone grease and was mixed for about 15 min. The MWCNTs were added at a weight fraction of 0.1 and 1%. The selection of low weight fraction was based on the fact that, large aspect ratio of CNTs makes it possible to achieve percolation at lower fractions [7]. The experiments were conducted at four loading conditions of no load, 2 kg, 5 kg and 10 kg.

## Results and discussion

Experiments were conducted to estimate heat flux transients for specimens with length to diameter ratio of 1. Figure 4, shows the variation of heat flux with time at various loading conditions for bare interfaces (without TIM) and for interfaces with silicone grease as TIM. In the present investigation, the peak heat flux under the no load condition was about  $17.52 \text{ kW m}^{-2}$ . The increase in the applied load to 2 kg resulted in the increase in peak heat flux substantially to a value of  $32.04 \text{ kW m}^{-2}$ . Further, increase in load from 2 kg to 5 kg resulted in the rise of peak heat flux value to  $48.53 \text{ kW m}^{-2}$ . This is due to the fact that as the load increases, the interfacial contact condition improves leading to enhanced heat transfer. The peak heat flux showed an increasing trend even as the load was increased to 10 kg. This trend of increase in peak heat flux with the increase in load was also reported by Kumar *et al* [25] in their studies for stainless steel contacts. The peak heat flux for 10 kg loading condition was estimated to be  $56.06 \text{ kW m}^{-2}$ .

The application of higher load for enhancing contact heat transfer is not an ideal solution particularly for the applications involving miniaturization. Hence, a more ideal approach is to introduce a TIM between two surfaces at contact. In the present work silicone grease was chosen as TIM because of its excellent wettability, stability and lower modulus [5]. Figure 4(b) shows the variation of heat flux with time at various loading conditions for Cu–Cu interface specimens with L/D ratio of 1 having silicone grease as TIM. For interfaces with silicone grease as TIM, the peak heat flux values for loading conditions of no load, 2 kg, 5 kg and 10 kg were found to be 31.71, 50.35, 64.86 and  $65.43 \text{ kW m}^{-2}$  respectively. Figures 5(a)–(d) shows the comparison of peak heat flux obtained for bare interfaces and for interfaces with silicone grease TIM. In each of the loading condition, the application of silicone grease as TIM resulted in an appreciable increase in peak heat flux. The application of TIM at the interface results in the replacement of air which is a poor conductor of heat. In addition to the higher thermal conductivity of silicone grease, excellent wettability, decrease in viscosity with





increased temperature and lower modulus aid in enhanced heat transfer as the TIM flows in to the voids that exist at the interface.

In addition to peak heat flux, the area under the heat flux transients was determined. This gives integral heat flow and is a quantitative measure of the heat transfer. Figures 6a and (b) show the variation in integral heat flow with time at different loading conditions for both bare interface and for interfaces with silicone grease as TIM. For the purpose of comparison, the integral curve for the first 100 s was plotted. The integral flow was calculated by using the following equation

$$Q = \int_0^t q dt \quad (8)$$

Where Q is the integral heat flow,

q is the heat flux

t is the time.

Figure 6(a) shows that in the case of bare interfaces, the area under the curve increases as the load is increased. The increase in the area under curve indicates that, at higher loads, the heat transferred to the lower specimen increases. Thus higher loading results in better conformance of the interfaces owing to the increase in the contact area. However, it is observed that for bare interfaces as the load increases, the percentage increase in heat flow across the interface decreases. The percentage increase in heat flow as the load increased from no load condition to 2 kg and further from 2 kg to 5 kg was about 62% and 40% respectively. However, the percentage increase in heat flow as the load was increased from 5 kg at 10 kg was only about 15.46%. This is attributed the fact that there is no much scope in increasing the contact area as the application of 5 kg load would have brought significant deformation leading to a better thermal contact at the interface. Figure 6(b) shows the variation in integral heat flow when silicone grease was used as TIM. The addition of silicone grease as TIM results in enhancement of heat across the specimen. From the graph and from the integral flow data shown in the Table 1,

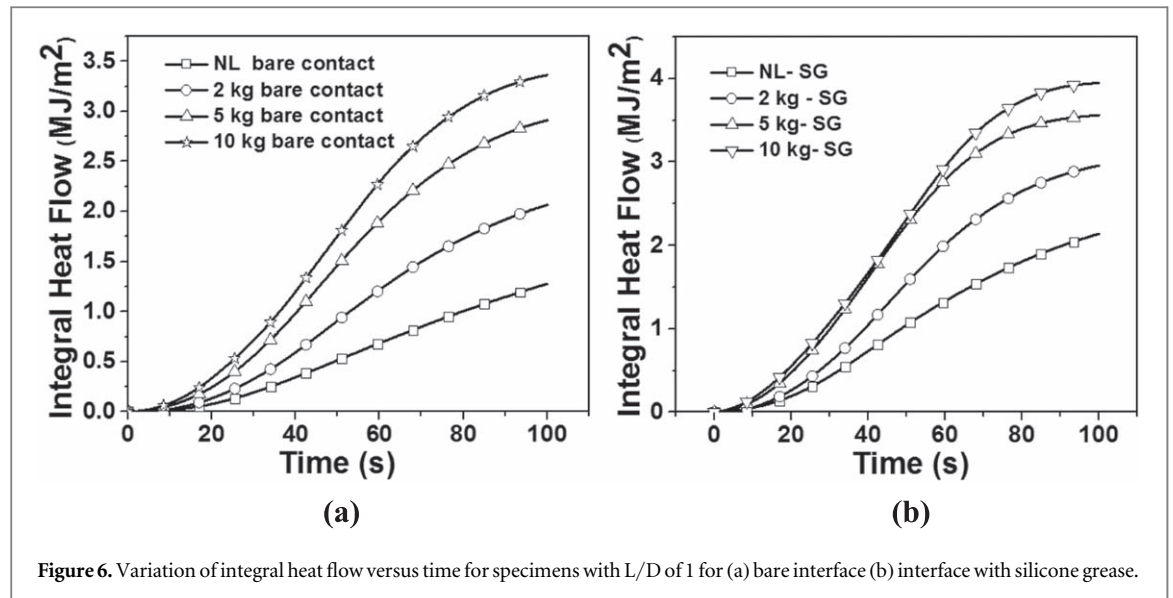


Figure 6. Variation of integral heat flow versus time for specimens with L/D of 1 for (a) bare interface (b) interface with silicone grease.

Table 1. Values of peak heat flux and integral heat flow for specimens with L/D ratio of 1.

Sl no	TIM/interface condition	Load (kg)	Peak heat flux ( $\text{kW m}^{-2}$ )	Integral flux ( $\text{MJ m}^{-2}$ )
1	bare contact	no load	17.52	1.27
2	bare contact	2	32.04	2.07
3	bare contact	5	48.53	2.91
4	bare contact	10	56.06	3.36
5	silicone grease	no load	31.71	2.13
6	silicone grease	2	50.35	2.95
7	Silicone grease	5	64.86	3.56
8	Silicone grease	10	65.43	3.94

it is evident that, under transient conditions, the application of silicone grease TIM increases heat flow across the interface. The percentage rise in heat flow was as high as 67% under no load condition and at higher load of 10 kg the increase was about 17.46%.

Experiments showed that for bare contacts, increasing the load from no load condition to 10 kg resulted in a rise of 164% in the integral heat flow value, whereas in the case of interfaces with silicone grease, an increase in the load from no load to 10 kg resulted in 84.97% rise in the value. This indicates that the effect of load on thermal contact resistance is significant when there is no use of TIM. In the presence of interface material, the effect of load on interfacial heat transfer is less significant.

In order to characterise heat transfer across the interface, a dimensionless temperature was defined.

The dimensionless temperature ( $\Theta$ ) was defined as,

$$\Theta = (T_{\max} - T_2) / (T_{\max} - T_i) \quad (9)$$

$T_2$  is the temperature at 3 mm below the interface in the lower specimen

$T_{\max}$  is the temperature to which the upper body is heated

$T_i$  is the initial temperature

The dimensionless temperature gives a qualitative account of the rate at which heat is extracted from the heat source to the heat sink. Figures 7(a) and (b) clearly show that for specimens with L/D ratio of 1, as the load increases the heat absorbed also increases. In the case of bare contacts, the time taken by heat sink to reach 50% of the maximum temperature is about 200 s under no load condition. Upon applying silicone grease the corresponding time taken reduces to about 100 s. When the load is increased to 10 kg in the case of bare interfaces, the time taken for the heat sink to reach 50% of the maximum temperature is about 80 s. The application of silicone grease for interfaces subjected to 10 kg load, the time taken to reach 50% the maximum temperature reduces to about 50 s. Thus, the study reveals that subjecting the interfaces with higher loads and the application of silicone grease as TIM results in faster extraction of heat. The faster heat transfer is attributed to the fact that as the load increases the number of contact point theoretically increases which results in greater establishment of link between upper body and lower body resulting in lower degree of air barrier. The lower degree of air barrier would result in faster propagation of heat across the interface. Further, the application of

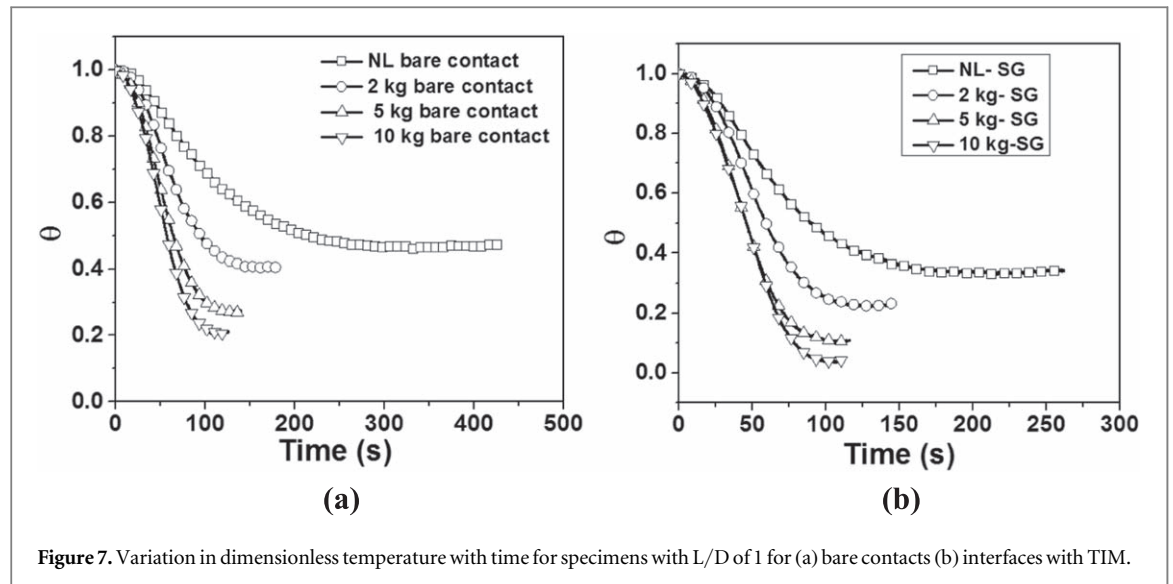


Figure 7. Variation in dimensionless temperature with time for specimens with L/D of 1 for (a) bare contacts (b) interfaces with TIM.

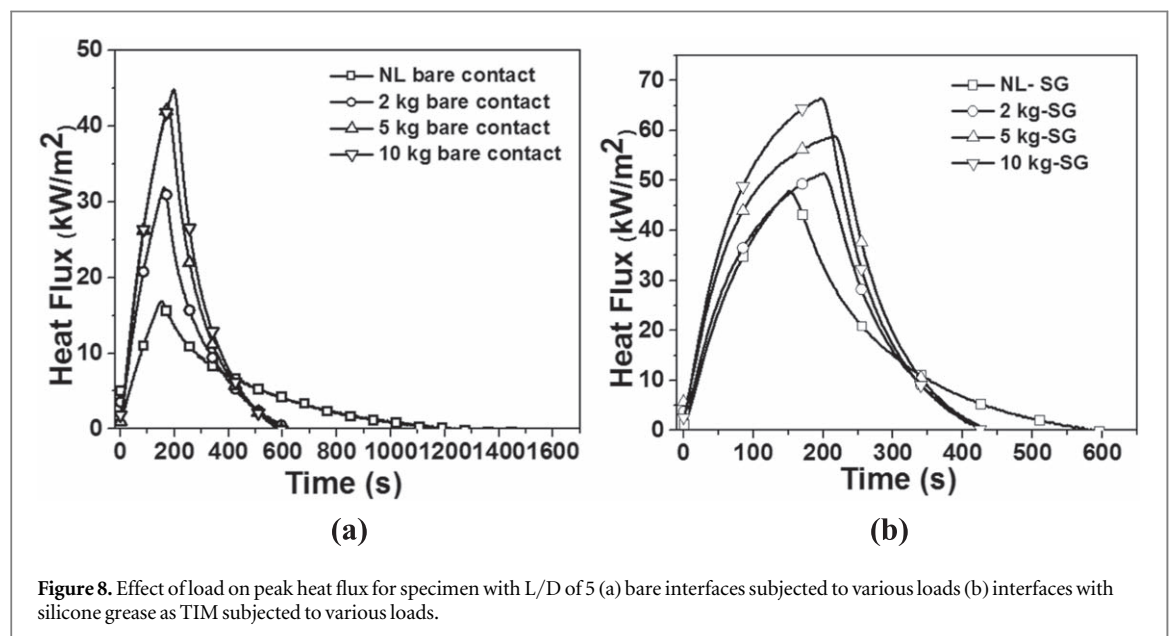


Figure 8. Effect of load on peak heat flux for specimen with L/D of 5 (a) bare interfaces subjected to various loads (b) interfaces with silicone grease as TIM subjected to various loads.

silicone grease as TIM would result in the source and sink material to be more contiguous physically, resulting in faster propagation of heat.

Experiments were also conducted for specimens with L/D ratio of 5. The variation in the heat flux values for bare interface and for interface with silicone grease is plotted in figures 8(a) and (b). With the increase in the load, the peak heat flux also increased. Similar trends were observed for specimens with L/D ratio of 1. The application of silicone grease as TIM resulted in enhancement of peak heat flux values. The peak heat flux values for no load, 2 kg, 5 kg and 10 kg for the interfaces with silicone grease as TIM were  $47.85 \text{ kW m}^{-2}$ ,  $51.42 \text{ kW m}^{-2}$ ,  $58.91 \text{ kW m}^{-2}$  and  $66.42 \text{ kW m}^{-2}$  respectively. Similarly, the corresponding peak heat flux for bare interfaces were  $16.83 \text{ kW m}^{-2}$ ,  $31.94 \text{ kW m}^{-2}$ ,  $42.60 \text{ kW m}^{-2}$  and  $44.84 \text{ kW m}^{-2}$  respectively.

Figures 9(a)–(d) shows the comparison of heat flux with time for bare and for interfaces with silicone grease as TIM for specimens with L/D ratio of 5. The application of silicone grease as TIM resulted in the rise in peak heat flux for each of the loading conditions. Thus, it can be concluded that the addition of pristine silicone grease as TIM results in increase in peak heat flux values irrespective of L/D ratio employed.

The determination of integral heat flow showed that with the application of silicone grease, there is a significant improvement in heat transfer across the interface. Also the integral heat flow was found to increase with the increase in load even for specimens with L/D ratio of 5. Figures 10(a) and (b) show the variation in the integral heat flow with time for interfaces with and without TIM. The integral curve for 400 s was plotted. The integral values are shown in Table 2 and were calculated using equation (8). For, bare interfaces, the increase in integral heat flow as the load was applied from no load condition to 2 kg and further from 2 kg to 5 kg resulted in

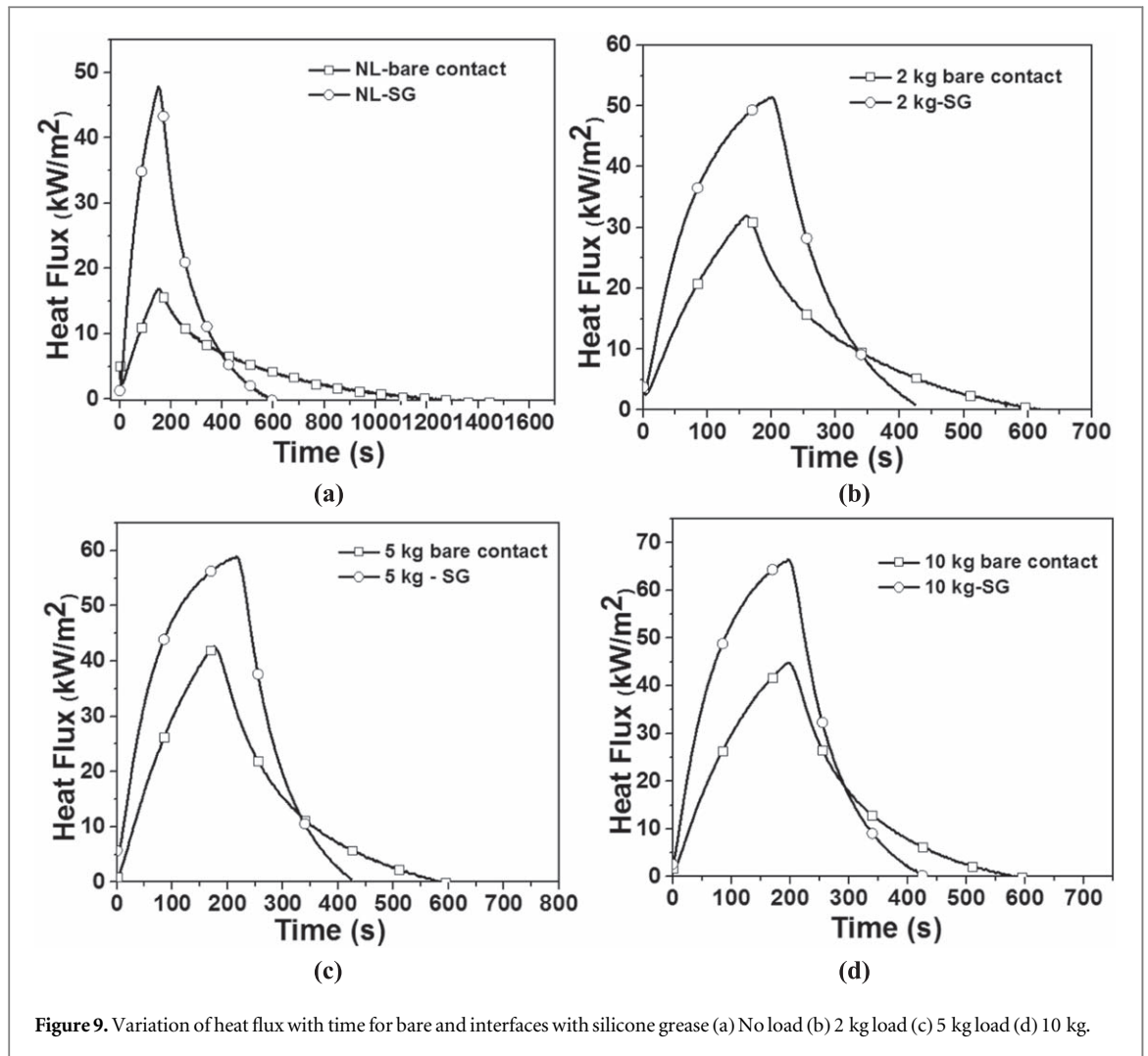


Figure 9. Variation of heat flux with time for bare and interfaces with silicone grease (a) No load (b) 2 kg load (c) 5 kg load (d) 10 kg.

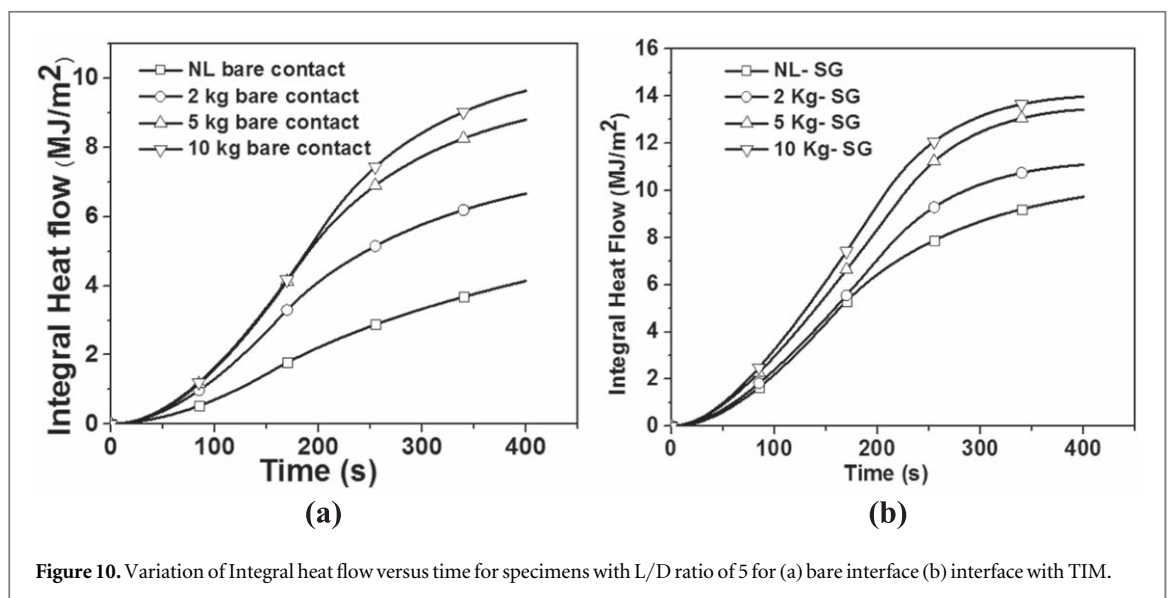
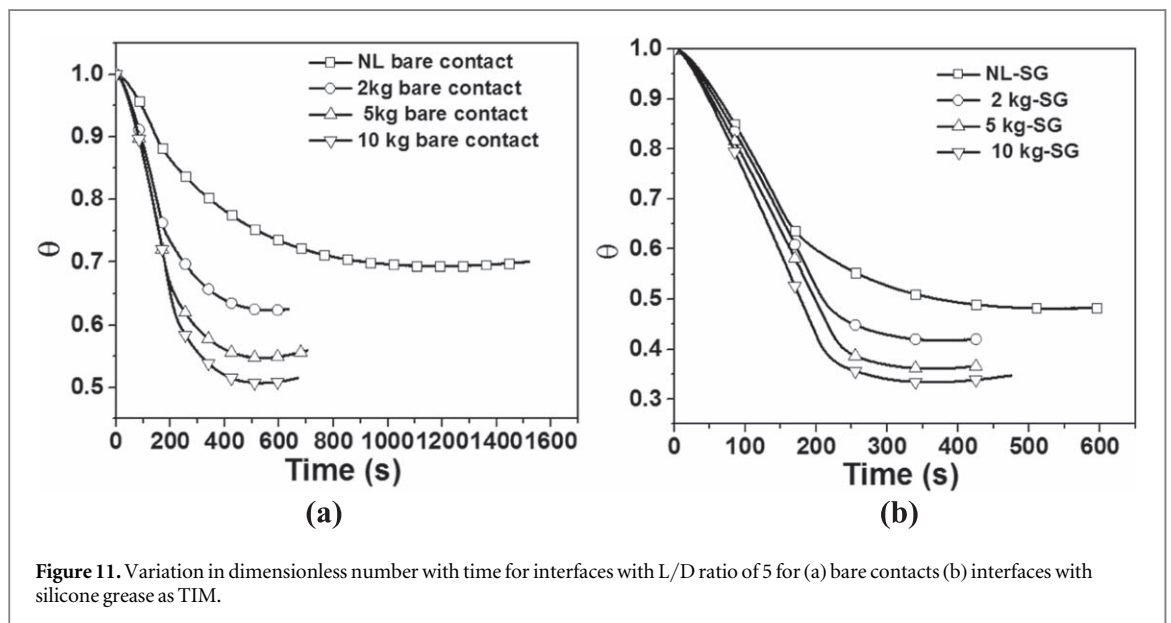


Figure 10. Variation of Integral heat flow versus time for specimens with L/D ratio of 5 for (a) bare interface (b) interface with TIM.

an increase of 61% and 32% respectively. Furthermore, increasing the load to 10 kg from 5 kg resulted in just over 9% in the values of integral heat flow. Similar trends were noticed in the case of L/D ratio of 5. The analysis of integral curve and peak heat flux reveals that addition of silicone grease as TIM results in efficient heat transfer across interfaces owing to the replacement of air with comparatively higher thermal conductive silicone grease TIM. The increase in integral heat flow was observed for all the loading conditions, with an increase as high as

**Table 2.** Values of peak heat flux and integral flux for specimens with L/D of 5.

Sl no	TIM/interface condition	Load (kg)	Peak heat flux (kW m <sup>-2</sup> )	Integral flux (MJ m <sup>-2</sup> )
1	bare contact	no load	16.83	4.13
2	bare contact	2	31.94	6.66
3	bare contact	5	42.60	8.80
4	bare contact	10	44.84	9.63
5	silicone grease	no load	47.85	9.72
6	silicone grease	2	51.42	11.07
7	silicone grease	5	58.91	13.42
8	silicone grease	10	66.42	13.96



135% for no load condition and an increase of 44% in case of applied load of 10 kg. For interfaces with silicone grease as TIM, increasing the load beyond 5 kg to 10 kg did not result in significant increase in the heat flow value. The possible reason has already been discussed for the case of specimens with L/D ratio of 1. The explanation also holds good for specimens with L/D ratio of 5.

The experiments also showed that in the case of specimens with L/D ratio of 5, for bare contacts, increasing the load from no load condition to 10 kg resulted in a rise of 133% in the integral heat flow value, whereas in the case of interfaces with silicone grease, an increase in the load from no load to 10 kg resulted in 43.62% rise in the value. This indicates that the effect of load on thermal contact resistance is significant when TIM was not used, even under the case of transient conditions.

The analysis of dimensionless temperature for specimens with L/D of 5 showed that, increasing the load and the application of TIM at the interfaces results in higher heat absorption by heat sinks (figures 11 (a) and (b)). For bare contacts, the time taken by the heat sink to reach 70% of the maximum temperature is about 700 s. However, with the application of silicone grease TIM, the heat sink took just around 180 s. As the load was increased to 10 kg for bare interfaces, the time taken by the heat sink to reach about 70% of the maximum temperature was about 200 s. However, as the load gets increased to 10 kg for interfaces with silicone grease about 70% of maximum temperature is attained by the heat sink by around 120 s. Hence it can be concluded that the load and the interface material has an effect on the conformance of the contacting surfaces. Similar effect was found in case of specimens with L/D ratio of 1.

The effect of the addition of MWCNTs to the interface material on contact heat transfer was investigated. Figure 12 shows the interfacial heat flux transients when silicone grease and MWCNT- Silicone grease were used as TIM for specimens with L/D ratio of 1. The values of peak heat flux and the area under integral curve for various loading and interface conditions are shown in table 3. In this case, the addition of 0.1 wt% MWCNTs – silicone grease at no load condition resulted in increased peak heat flux value of 52.62 kW m<sup>-2</sup>. Thus, the addition of MWCNTs resulted in a significant rise in peak heat flux as compared to the peak heat flux value of

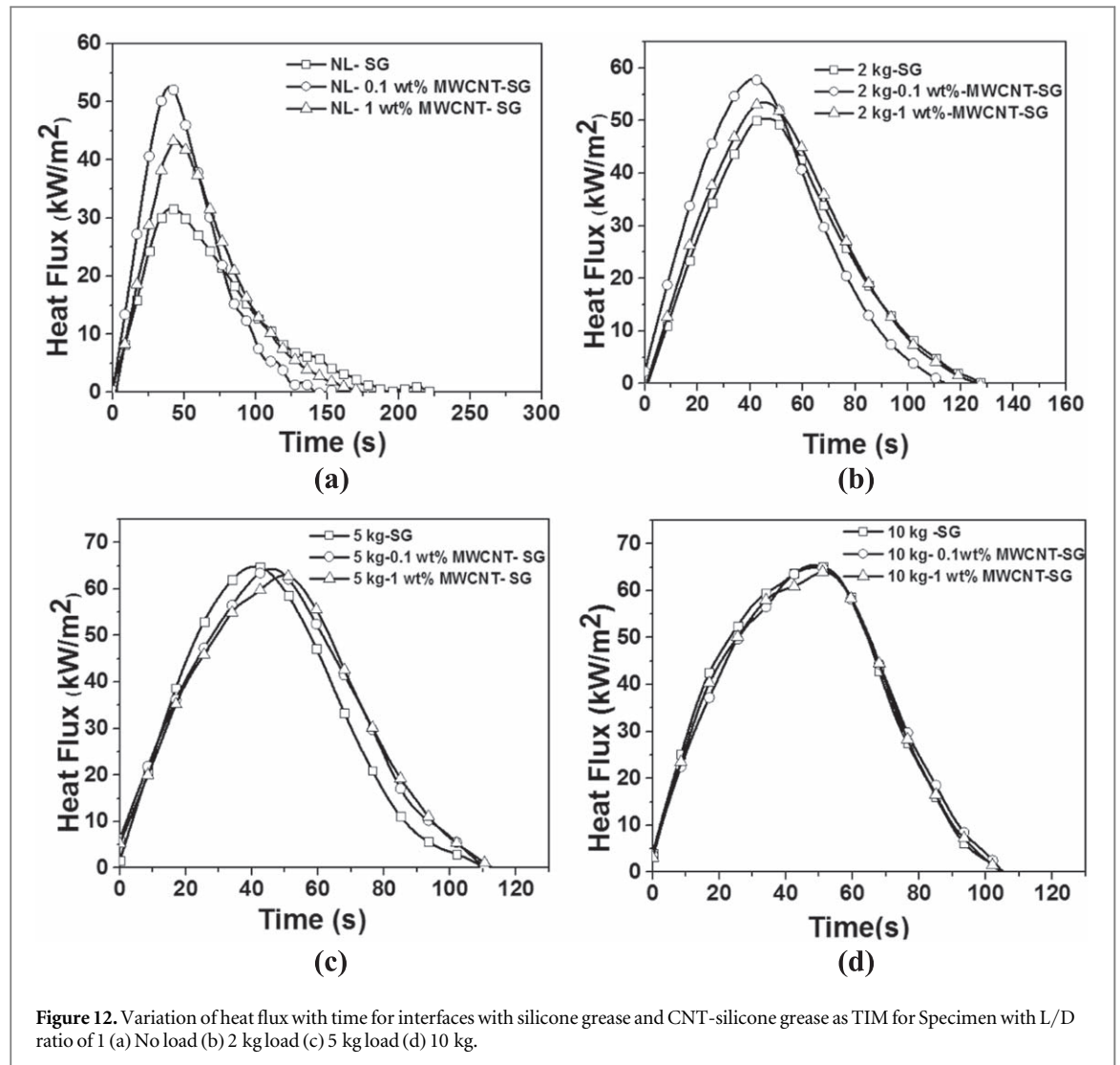


**Figure 12.** Variation of heat flux with time for interfaces with silicone grease and CNT-silicone grease as TIM for Specimen with L/D ratio of 1 (a) No load (b) 2 kg load (c) 5 kg load (d) 10 kg.

**Table 3.** Peak heat flux and area under curve for specimens with L/D of 1.

Sl no	TIM	Load (kg)	Peak heat flux ( $\text{kW m}^{-2}$ )	Area under curve ( $\text{MJ m}^{-2}$ )
1	Pristine silicone grease	no load	31.71	2.13
2	silicone grease with 0.1 wt % MWCNT	no load	52.62	2.97
3	silicone grease with 1 wt % MWCNT	no load	43.47	2.66
4	Pristine silicone grease	2	50.35	2.95
5	silicone grease with 0.1 wt % MWCNT	2	57.94	3.21
6	silicone grease with 1 wt % MWCNT	2	53.50	3.15
7	Pristine silicone grease	5	64.86	3.56
8	silicone grease with 0.1 wt % MWCNT	5	64.33	3.78
9	silicone grease with 1 wt % MWCNT	5	62.86	3.76
10	Pristine silicone grease	10	65.43	3.94
11	silicone grease with 0.1 wt % MWCNT	10	64.96	3.89
12	silicone grease with 1 wt % MWCNT	10	63.87	3.87

31.71  $\text{kW m}^{-2}$  when pristine silicone grease was used as TIM. Further, increasing the weight fraction to 1% resulted in the peak heat flux dipping to a lower value of 43.47  $\text{kW m}^{-2}$ . The integral flow values also showed similar increasing trend when 0.1 wt% MWCNTs were added for no load condition. Further, the integral flow dipped as the weight fraction of MWCNTs was increased to 1 wt%. In fact, the integral flow deteriorated for all loading conditions as 1 wt% MWCNT—silicone grease was used as TIM as compared to 0.1 wt%-MWCNT-Silicone grease. Figure 13 shows the corresponding heat flux transients for specimens with L/D ratio of 5. For no load condition, the addition 0.1 MWCNTs to silicone grease resulted in increase in peak heat flux and the

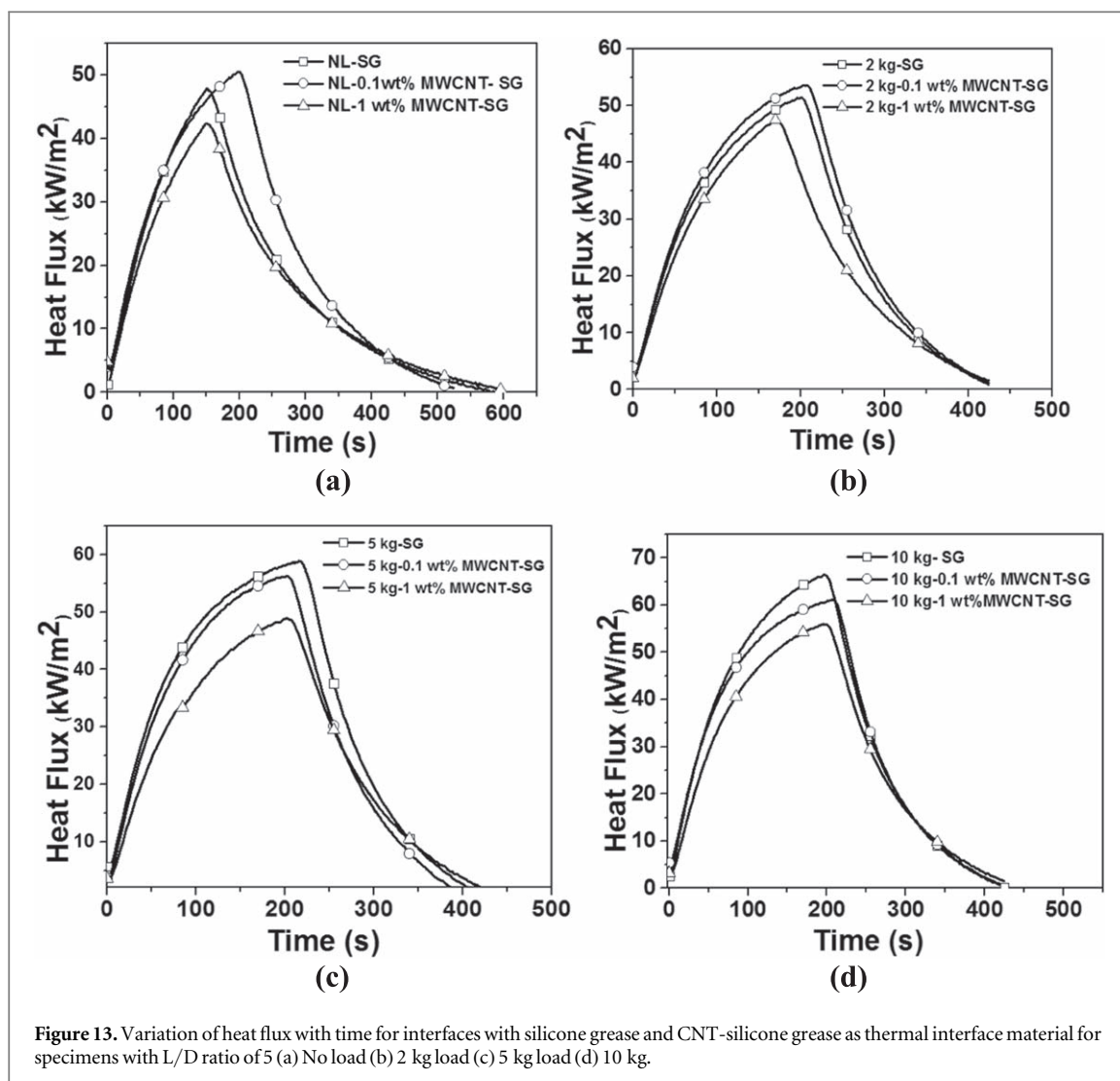
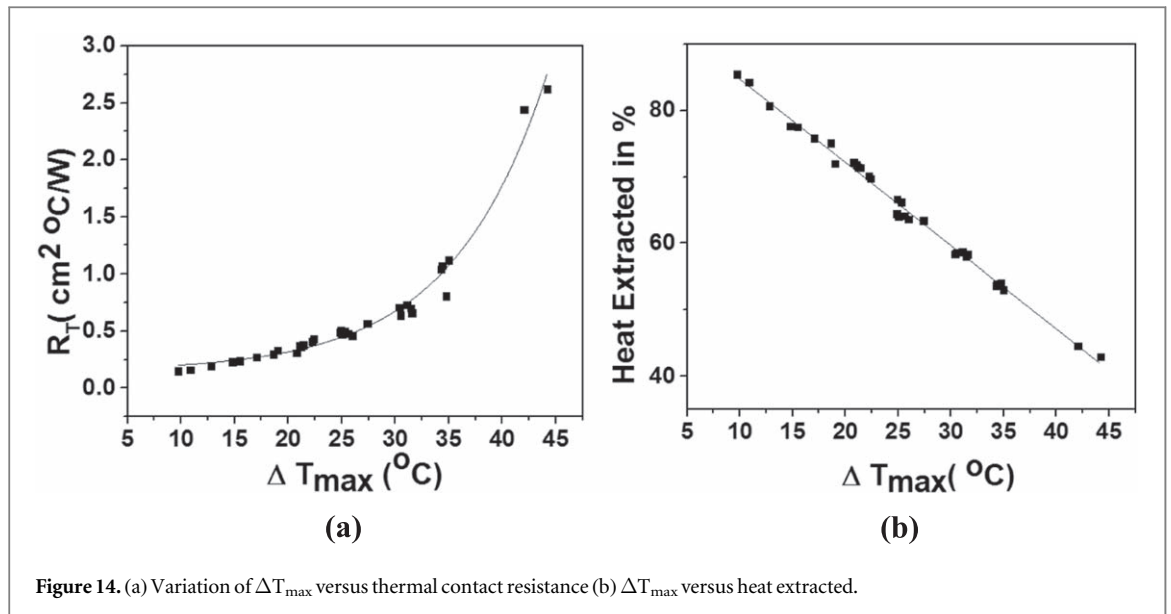


**Figure 13.** Variation of heat flux with time for interfaces with silicone grease and CNT-silicone grease as thermal interface material for specimens with L/D ratio of 5 (a) No load (b) 2 kg load (c) 5 kg load (d) 10 kg.

**Table 4.** Peak heat flux and area under curve for specimens with L/D of 5.

Sl no	TIM	Load (kg)	Peak heat flux (kW m <sup>-2</sup> )	Area under curve (MJ m <sup>-2</sup> )
1	Pristine silicone grease	no load	47.85	9.72
2	silicone grease with 0.1 wt% MWCNT	no load	50.53	11.49
3	silicone grease with 1 wt% MWCNT	no load	42.34	8.88
4	Pristine silicone grease	2	51.42	11.07
5	silicone grease with 0.1 wt% MWCNT	2	53.59	11.80
6	silicone grease with 1 wt% MWCNT	2	47.49	9.54
7	Pristine silicone grease	5	58.91	13.42
8	silicone grease with 0.1 wt% MWCNT	5	56.26	12.13
9	silicone grease with 1 wt% MWCNT	5	48.96	10.82
10	Pristine silicone grease	10	66.42	13.96
11	silicone grease with 0.1 wt% MWCNT	10	61.11	13.54
12	silicone grease with 1 wt% MWCNT	10	55.97	12.05

integral heat flow. Table 4 shows the values of peak heat flux and integral heat flow values across interface for specimens with L/D ratio of 5. The study found that the addition of MWCNT to silicone grease at 0.1 wt% resulted in enhancement of heat flow. This could be attributed to the ability of MWCNTs to attain percolation at lower fractions [7]. However, the heat flow deteriorated at higher loads. Further, increase in the MWCNT fraction to 1 wt% resulted in decrease in heat flow values under all loading conditions. It is clear from the experiments that the addition of silicone based TIMs increases the heat transfer across the interface. The results also indicate that, MWCNT impregnated silicone grease with 0.1 wt% shows superior performance when compared to the silicone grease with 1 wt% MWCNTs. The possible explanation for the deterioration could be



based on rheology of the Particle laden polymer TIMs [16]. Based on the findings of Prasher et al [16], it was assumed that the MWCNT based silicone greases follow Non-Newtonian behaviour owing to the addition of MWCNTs in to the matrix. Further, we assume that the one dimensional structure of MWCNTs [7] helps in achieving percolation at lower MWCNT fractions. It has been reported in the literature [16] that higher volume fraction of particles results in increased viscosity leading to higher yield stress which decreases the spreadability of TIMs employed [16,24]. Thus increase in MWCNTs from a weight fraction of 0.1 to 1% results in enhancement of the resistance for heat transfer. Frabis *et al* [24] in their study also noted that increasing the CNT results in formation of paste that is thick and difficult to spread.

To compare the effect of L/D ratio on heat flow,  $R_T$  (thermal contact resistance) versus  $\Delta T_{\max}$  was plotted. Figure 14(a) shows the variation of  $R_T$  with maximum temperature difference ( $\Delta T_{\max}$ ) for both specimens of L/D ratio of 1 and 5. The analysis shows that, as the maximum temperature difference between the upper specimen and lower specimen increases, the thermal contact resistance also increases exponentially. From the figure 14(b) it is evident that with the increase in the maximum temperature difference, the heat extracted by the lower specimen also decreases. The study reveals that thermal contact resistance depends on  $\Delta T_{\max}$  for all interfacial conditions irrespective of L/D ratio used. The future studies could focus on the effect of surface roughness, rheological properties of TIMs, mechanical properties of the source and sink and suitability of other types of TIMs on the thermal contact heat transfer thus enabling design engineers to have better insights on parameters affecting heat transfer across interfaces.

## Conclusion

In the present investigation, the effect of L/D ratio of hot and cold cylindrical copper specimens on interfacial heat flux under transient conditions was studied. It was found that for both length to diameter ratios of 1 and 5, there exists a threshold load of 5 kg beyond which the increase in heat flow parameters was not significant. The study also found that the introduction of various silicone grease based TIMs under transient conditions resulted in the enhancement of heat transfer. The impregantaion of MWCNTs to silicone grease in lower concentrations resulted in enhancement of heat flux transients and thermal performance at lower loads, irrespective of the L/D ratios employed. Based on experimental findings, it was concluded that the thermal performance of 0.1 wt% MWCNT-SG TIM was superior when compared to 1 wt% MWCNT-SG TIM. The thermal contact resistance exponentially increased with peak temperature difference irrespective of the L/D ratio employed.

## ORCID iDs

K NarayanPrabhu  <https://orcid.org/0000-0002-8359-2587>



## References

- [1] Khan M F and Balandin A A 2012 Graphene–multilayer graphene nanocomposites as highly efficient thermal interface materials *Nano Lett.* **12** 861–7
- [2] Raza M A, Westwood A and Stirling C 2015 Comparison of carbon nanofiller-based polymer composite adhesives and pastes for thermal interface applications *Mater. Des.* **85** 67–75
- [3] Sartre V and Lallemand M 2001 Enhancement of thermal contact conductance for electronic systems *Appl. Therm. Eng.* **21** 221–35
- [4] Macris C G, Thomas R S, Ebel R G, Leyerle C B and Solutions E 2004 Performance, reliability, and approaches using a low melt alloy as a thermal interface material *Proc. IMAPS (37th International Symposium on Microelectronics) (Long Beach California United States of America, November 14-18)* (<https://doi.org/10.1109/ESTC.2006.280178>)
- [5] Becker G, Lee C and Lin Z 2005 Thermal conductivity in advanced chips: emerging generation of thermal greases offers advantages *Advanced Packaging* **14** 14
- [6] Gwinn J P and Ralph L W 2003 Performance and testing of thermal interface materials *Microelectron. J.* **34** 215–22
- [7] Hansson J, Torbjörn M J N, Ye L and Liu J 2018 Novel nanostructured thermal interface materials: a review *Int. Mater. Rev.* **63** 22–45
- [8] Abdullah M Z, Yau Y C, Zainal Alauddin Z A and Seetharamu K N 2001 Effects of pressure on thermal contact resistance for rough mating surfaces *ASEAN Journal on Science and Technology for Development* **18** 29–35
- [9] Roy C K, Bhavnani S, Hamilton M C, Johnson R W, Knight R W and Harris D K 2016 Thermal performance of low melting temperature alloys at the interface between dissimilar materials *Appl. Therm. Eng.* **99** 72–9
- [10] Tariq A and Asif M 2016 Experimental investigation of thermal contact conductance for nominally flat metallic contact *Heat Mass Transfer* **52** 291–307
- [11] Liu Z and Chung D D 2006 Boron nitride particle filled paraffin wax as a phase-change thermal interface material *J. Electron. Packag.* **128** 319–23
- [12] Yovanovich M, Culham J and Teertstra P 1997 Calculating interface resistance *Electronics Cooling, May issue* **3** 24–29
- [13] Yu W, HuaqingXie L, Chen Z, Zhu J, Zhao and Zhang Z 2014 Graphene based silicone thermal greases *Phys. Lett. A* **378** 207–11
- [14] Sarvar F, David C W and Conway P P 2006 Thermal interface materials-a review of the state of the art 2006 *1st Electronic Systemintegration Technology Conf. 2 (Dresden, Germany)* (IEEE) pp 1292–1302
- [15] Yujun G, Zhongliang L, Guangmeng Z and Yanxia L 2014 Effects of multi-walled carbon nanotubes addition on thermal properties of thermal grease *Int. J. Heat Mass Transfer* **74** 358–67
- [16] Prasher R S, Shipley J, Prstic S, Koning P and Wang J-lin 2003 Thermal resistance of particle laden polymeric thermal interface materials *J. Heat Transfer* **125** 1170–1177
- [17] Prasher R 2006 Thermal interface materials: historical perspective, status, and future directions *Proc. IEEE* **94** 1571–86
- [18] Zhao J-W, Zhao R, Huo Y-K and Cheng W-L 2019 Effects of surface roughness, temperature and pressure on interface thermal resistance of thermal interface materials *Int. J. Heat Mass Transfer* **140** 705–16
- [19] Otiaba K C, Ndy N E, Bhatti R S, Mallik S, Alam M O and Amalu E H 2011 Thermal interface materials for automotive electronic control unit: trends, technology and R&D challenges *Microelectron. Reliab.* **51** 2031–43
- [20] Yu W, Xie H, Yin L, Zhao J, Xia L and Chen L 2015 Exceptionally high thermal conductivity of thermal grease: synergistic effects of graphene and alumina *Int. J. Therm. Sci.* **91** 76–82
- [21] Blazej D Thermalinterfacematerial <https://electronicscooling.com/2003/11/thermal-interface-materials/> (<https://doi.org/10.1016/j.microre.2011.05.001>)
- [22] Gowda et al 2005 Reliability testing of silicone-based thermal greases [IC cooling applications] *Semiconductor Thermal Measurement and Management IEEE Twenty First Annual IEEE Symp., 2005* pp 64–71 (Piscataway, NJ) (IEEE)
- [23] Hongyuan C, Wei H, Chen M, Meng F, Li H and Li. Q 2013 Enhancing the effectiveness of silicone thermal grease by the addition of functionalized carbon nanotubes *Appl. Surf. Sci.* **283** 525–31
- [24] Fabris D, Rosshirt M, Cardenas C, Wilhite P, Yamada T and Yang C Y 2011 Application of carbon nanotubes to thermal interface materials *J. Electron. Packag.* **133** 020902
- [25] Kumar S and Tariq A 2017 Determination of thermal contact conductance of flat and curvilinear contacts by transient approach *Exp. Therm Fluid Sci.* **88** 261–76
- [26] Narayan Prabhu K and Ashish A A 2002 Inverse modeling of heat transfer with application to solidification and quenching *Mater. Manuf. Processes* **17** 469–81
- [27] Stolz G 1960 Numerical solutions to an inverse problem of heat conduction for simple shapes *J. Heat Transfer* **82** 20–5
- [28] Beck J V 1970 Nonlinear estimation applied to the nonlinear inverse heat conduction problem *Int. J. Heat Mass Transfer* **13** 703–16